Chapter 4

Wavelet collocation approaches for partial differential equations

Contents

4.1 Introduction

PDE solutions using wavelet algorithms are usually based on Galerikin techniques as given by Chen, C. Hwang, Y. P. Shih [106], Vani [8] or collocation methods by Naldi [97], [108]. Daubechies wavelets were used in most of the cases.

M.Q. Chen, C. Hwang, Y. P. Shih [106] used Daubechies wavelet for implementing wavelet Galerikin approach on a bounded interval. The exact evaluation of various finite integrals, whose integrands involved products of Daubechies compactly supported wavelets and their derivatives and/or integrals.

Wavelet Galerikin scheme involves the evaluation of connection coefficients. Connection coefficients are integrals with integrand being the product of wavelet bases and their derivatives.

Valeriano Comincioli, Naldi [108] solved the evolution equation using an adaptive wavelet algorithm. They implemented Daubechies wavelet along with a two stage implicit Runge Kutta method with a suitable numerical approximation of the exact Jacobian. They implemented the approach to a one dimensional semilinear parabolic equation given by,

$$w_t = w_{xx} + f(w), \quad w(x,0) = w_0$$

and specified boundary conditions. It was solved after reformulating it to an abstract Cauchy problem in L^2 space as,

$$W' = AW + F(w), \quad W(0) = W^0$$

where the boundary conditions together with the differential operators were incorporated into the operator A.

As explicit expression for Daubechies wavelets are not available so their analytical differentiation or integration is not possible. This fact in particular complicates the solution of nonlinear PDE's, where integrals of products of wavelets and their derivatives must be computed. This can be done by introducing the connection coefficients as given by Juan [46], which is possible only for a few class of nonlinearities. But numerical evaluation of these coefficients is often unstable or inaccurate [103]. So Haar wavelet(db1) being piecewise constant function is utilized to overcome these shortfalls.

Evolution equations were solved by Lepik [103] using Haar approximation. Boundary layer fluid flow problem was solved using Haar by Siraj-ul-Islam, Sarler B., Aziz I. and Fazal-i-Haq [95].

They had solved natural convection bounday layer flow. The natural convection flows are caused by the density gradient. Density variation is caused due to the temperature difference. The governing PDE consist of continuity, momentum and energy of two dimensional flow over a vertical flat plate with uniform surface temperature given by,

$$\frac{\partial u}{\partial x} + \frac{\partial v}{\partial y} = 0$$

$$u\frac{\partial u}{\partial x} + v\frac{\partial v}{\partial y} = \gamma\frac{\partial^2 u}{\partial y^2} + g\beta\frac{T - T_\infty}{T_W - T_\infty}$$

$$u\frac{\partial T}{\partial x} + v\frac{\partial T}{\partial y} = \alpha\frac{\partial^2 T}{\partial y^2}$$

subject to the boundary conditions,

$$y = 0: \quad u = 0, \quad v = 0, \quad T = T_W(x)$$

$$y \to \infty : \quad u = 0, \quad T = T_\infty$$

where x and y are coordinates measured parallel and perpendicular to the plate. They had transformed the PDE to a system of nonlinear ODE's, then applied Haar wavelet algorithm for the system of ODE.

Lepik [102] solved the evolution equation,

$$\alpha \frac{\partial^2 u}{\partial t^2} + \beta \frac{\partial u}{\partial t} = F(t, u, \frac{\partial u}{\partial x}, \frac{\partial^2 u}{\partial x^2}),$$

where $t \in [t_{in}, t_{fin}], \quad x \in [x_{in}, x_{fin}]$.

He took F to be a nonlinear function along with $\alpha, t_{in}, t_{fin}, x_{in}, x_{fin}$ as constants. Dividing the interval $[t_{in}, t_{fin}]$ into N equal parts of length $\Delta t = \frac{(t_{in} - t_{fin})}{N}$ and denoting $t_s = (s-1)\Delta t, \quad s = 1, 2, ..., N$.

For subinterval $t \in [t_s, t_{s+1}]$ the solution is approximated. He considered the assumption of derivative of the solution as Haar series approximation in space as,

$$\dot{u''} = \sum_{n=0}^{m-1} c_s(n) h_n(x) \tag{4.1.1}$$

where c_s is a $2m$ dimensional row vector it is regarded as a vector constant in the subinterval $t \in [t_s, t_{s+1}]$. We extend Lepik's [103] to solve the parabolic equation with Haar approximation in one dimension and then extend the idea to solve the elliptic partial differential equations. Algorithms for the approach is described in detail along with five test problems. Brief tables describing the formulated results are given.

The implementation of Haar wavelet function as basis for solving ODE motivates its implementation to PDE. The initial attempt was done to utilize the basis function for approximating space variable in a parabolic equation. In the solution procedure of elliptic PDE the approximation was taken both in x and y space. Simple examples

were solved using codes generated to evaluate and solve the PDE.

4.2 Parabolic partial differential equation

To apply the proposed method we follow the following stages

- Function approximation.
- Subsequent integration depending on the order of the equation.
- Substitution of the values to the partial differential equation.
- Solving the system for Haar coefficients which leads to the solution.

Motivated by the concept similar to the considerations for an ordinary differential equation [102].
Considering an equation of the form $u_t = u_{xx}$ with particular initial and boundary condition, we recall equation 4.1.1, with $\dot{u''}$ representing first derivative with respect to time and second derivative with x, also

$$C_m{}^T = [c_0, c_1, ..., \ c_{m-1}] \quad and \quad h_m(x) = [h_0(x), h_1(x), ..., h_{m-1}(x)]^T$$

c_i represents Haar coefficients, $i = 0, 1, 2, .., (m-1)$ and $h_m(x)$ are Haar functions with
$m = 2^J$, where

$$\dot{u''} = \sum_{n=0}^{m-1} c_s(n) h_n(x) = C_m{}^T h_m(x), \tag{4.2.1}$$

where ${C_m}^T$ is a constant in $t \in (t_s, t_{s+1})$. Integrating the equation 4.2.1 with respect to t from t_s to t and twice with respect to x from 0 to x we obtain,

$$u''(x,t) = (t - t_s){C_m}^T h_m(x) + u(x, t_s) \tag{4.2.2}$$

$$\begin{aligned} u(x,t) = (t - t_s){C_m}^T Q_m(x) + x[u'(0,t) - u'(0,t_s)] \\ + u(0,t) - u(0,t_s) + u(x,t_s), \end{aligned} \tag{4.2.3}$$

where $Q_m(x)$ represents double integral of Haar function with respect to x from 0 to x. To utilize the boundary conditions

$$\begin{aligned} u(0,t_s) = g_0(t_s) \qquad u(1,t_s) = g_1(t_s) \\ \dot{u}(0,t) = {g_0}'(t) \qquad \dot{u}(1,t) = {g_1}'(t) \end{aligned} \tag{4.2.4}$$

we differentiate equation 4.2.3 with respect to t and put $x = 1$ to use equation 4.2.4 and obtain

$$\begin{aligned} u(1,t) = (t - t_s)C_m^T Q_m(x) + u(1,t_s) - u(0,t_s) \\ + u'(0,t) - u'(0,t_s) + u(0,t) \end{aligned} \tag{4.2.5}$$

$$\dot{u}(1,t) = C_m^T Q_m(x) + \dot{u}'(0,t) + \dot{u}(0,t) \tag{4.2.6}$$

$$\dot{u}(x,t) = C_m^T Q_m(x) + x\dot{u}'(0,t) + \dot{u}(0,t) \tag{4.2.7}$$

Rearranging equation we obtain

$$\begin{aligned} u'(0,t) - u'(0,t_s) = -(t-t_s)C_m^T Q_m(x) - u(1,t_s) \\ + u(0,t_s) - u(0,t) + u(1,t) \end{aligned} \tag{4.2.8}$$

$$\dot{u}'(0,t) \quad = \quad \dot{u}(1,t) - C_m^T Q_m(x) - \dot{u}(0,t) \tag{4.2.9}$$

Now taking $x \to x_l \quad and \quad t \to t_{s+1}$ and discretizing the result we obtain from equation 4.2.3

$$\begin{aligned} u(x_l,t_{s+1}) = (t_{s+1}-t_s){C_m}^T Q_m(x) + x[u'(0,t_{s+1}) - u'(0,t_s)] \\ + u(0,t_{s+1}) - u(0,t_s) + u(x,t_s) \end{aligned} \tag{4.2.10}$$

Using the equation 4.2.5 we get

$$\begin{aligned} u'(0,t_{s+1}) - u'(0,t_s) = -(t_{s+1}-t_s)C_m^T Q_m(x) - u(1,t_s) + u(0,t_s) \\ - u(0,t_{s+1}) + u(1,t_{s+1}) \end{aligned} \tag{4.2.11}$$

$$\dot{u}'(0,t_{s+1}) = \dot{u}(1,t_{s+1}) - C_m^T Q_m(x) - \dot{u}(0,t_{s+1}) \tag{4.2.12}$$

From equation 4.2.2 and equation 4.2.6 we obtain

$$\dot{u}(x_l,t_{s+1}) = C_m^T Q_m(x_l) + x_l[\dot{u}'(0,t_{s+1})] + \dot{u}(0,t_{s+1}) \tag{4.2.13}$$

$$u''(x_l,t_{s+1}) = (t_{s+1}-t_s)C_m^T h_m x_l + u''(x_l,t_s) \tag{4.2.14}$$

Hence from equation 4.2.10 using equations 4.2.11, 4.2.12, 4.2.13 and 4.2.9 we get

$$\begin{aligned} u(x_l, t_{s+1}) &= (t_{s+1} - t_s)C_m^T Q_m(x_l) + u(x_l, t_s) \\ &\quad - u(0, t_s) + x_l[-(t_{s+1} - t_s)C_m^T Q_m(x_l) \\ &\quad + u(1, t_{s+1}) - u(1, t_s) + u(0, t_s) \\ &\quad - u(0, t_{s+1})] + u(0, t_{s+1}) \end{aligned} \tag{4.2.15}$$

$$\begin{aligned} \dot{u}(x_l, t_{s+1}) &= C_m^T Q_m(x_l) + x_l[-C_m^T Q_m(x_l) - \dot{u}(0, t_{s+1}) \\ &\quad + \dot{u}(1, t_{s+1})] + \dot{u}(0, t_{s+1}) \end{aligned} \tag{4.2.16}$$

4.3 Numerical example

Consider a simple example

$$\begin{aligned} & & u_t &= u_{xx} \\ \textit{with} \quad \textit{condition} \quad & & u(x, 0) &= \sin(\pi x) \\ & & u(0, t) &= 0 \quad \textit{and} \quad u(1, t) = 0. \end{aligned} \tag{4.3.1}$$

Substituting the expression for derivative with t as in equation 4.2.13 and twice derivative with x in equation 4.2.14, system of equations are generated and they are solved to obtain Haar coefficients. The Haar coefficients are substituted in equation 4.2.15 which gives Haar solution. The solution using Haar wavelet collocation method is obtained using computer coding which is compared with solution obtained using analytic solution and finite difference method. The analytic solution

Table 4.1: Represents the absolute error between Haar solution and analytic with $J = 2$

x\t	x=0.0625	0.1875	0.3125	0.4375	0.5625	0.6875	0.8125	0.9375
t=0.0001	0.0001323	0.0001359	0.0001355	0.0001356	0.0001356	0.0001355	0.0001359	0.0001321
0.005	0.005168	0.002286	0.0032153	0.0032243	0.0032121	0.0030481	0.0007266	0.0146834
0.01	0.0103493	0.002762	0.0057416	0.0061405	0.0060397	0.0050278	0.0004646	0.0195367
0.015	0.0154442	0.0020657	0.0074223	0.0085369	0.0082825	0.0061571	0.0015896	0.0209419
0.05	0.0461981	0.0138149	0.0043511	0.0123356	0.013174	0.0083376	0.0017236	0.0164513
0.1	0.0757318	0.0401328	0.0154609	0.0007081	0.0056727	0.0053065	0.0002901	0.0096614
0.2	0.1026435	0.0734385	0.0493779	0.0309346	0.0180237	0.0101218	0.0063804	0.005714
0.65	0.0926572	0.078788	0.0651544	0.0519291	0.039268	0.027308	0.0161676	0.005951
0.9999	0.0687896	0.0584033	0.0481632	0.0382116	0.0286908	0.0197421	0.0115057	0.004122

for equation 4.3.1 obtained by variable separable method is,

$$u(x,t) = \sum_{m=1}^{\infty} b_m \sin(m\pi x) e^{-m^2\pi^2 t} \tag{4.3.2}$$

where

$$b_m = 2\int_0^1 \sin(m\pi x)\sin(\pi x)dx$$

$$b_1 = 1, \quad b_i = 0 \quad for \quad i = 2, 3, ...$$

$$u(x,t) = \sin(\pi x)e^{-\pi^2 t}$$

The absolute errors are listed in table 4.1 for space step taken with resolution of $J = 2$ and table 4.2 represents resolution of $J = 4$ with time step 0.0001. The solution improves with increased resolution which is clearly shown by reduced absolute error in the table 4.1 and 4.2.

Table 4.3 gives absolute error between the analytic solution and finite difference

Table 4.2: Represents the absolute error between Haar solution and analytic with $J = 4$

t\x	0.015625	0.046875	0.078125	0.265625	0.296875	0.328125	0.390625	0.671875	0.703125	0.890625	0.984375
t=0.0001	3.44E-05	4.48E-05	4.46E-05	4.49E-05	4.49E-05	4.5E-05	4.5E-05	4.5E-05	4.49E-05	4.47E-05	3.41E-05
0.005	0.001488	0.000825	0.000392	0.000128	0.000127	0.000125	0.000121	0.000122	0.00012	0.000481	0.001916
0.01	0.002948	0.001957	0.001212	0.000222	0.000252	0.000266	0.000274	0.000239	0.000208	0.000713	0.001889
0.015	0.004347	0.003126	0.002153	0.000195	0.000285	0.000341	0.000395	0.000308	0.000248	0.000785	0.001821
0.1	0.019826	0.017767	0.015836	0.006992	0.005941	0.004999	0.003414	0.000117	3.39E-05	0.00029	0.000775
0.2	0.026338	0.024613	0.022939	0.014184	0.012955	0.011793	0.00967	0.003195	0.002747	0.000909	0.000398
0.65	0.023764	0.0229	0.022037	0.01693	0.016095	0.015268	0.013635	0.006754	0.006046	0.002084	0.000301
0.9999	0.01804	0.017381	0.016722	0.012814	0.012174	0.011539	0.010286	0.005017	0.004479	0.00151	0.000213

Table 4.3: Represents the absolute error between analytic solution and finite difference method.

t\x	x=0.015625	0.046875	0.078125	0.265625	0.296875	0.328125	0.671875
t=0.0001	0.02897	0.067661	0.066682	0.048075	0.043131	0.037772	0.03205
0.005	0.046705	0.139665	0.231281	0.705274	0.764533	0.816429	0.81578
0.01	0.044456	0.13294	0.220144	0.671315	0.727721	0.777118	0.777118
0.015	0.042316	0.126539	0.209544	0.638991	0.692681	0.739699	0.739699
0.05	0.029956	0.089579	0.148339	0.452349	0.490357	0.523642	0.523642
0.1	0.018288	0.054688	0.090561	0.276158	0.299362	0.319682	0.319682
0.9999	2.54E-06	7.6E-06	1.26E-05	3.84E-05	4.16E-05	4.44E-05	4.44E-05

method with same step length of t as 0.0001 and step length of x taken as considered in Haar formulation with $J = 4$. The table clearly shows the improved solution pattern of Haar collocation method with reduced error as in Table 4.2

Here resolution $J = 2$ was considered for figure 4.1 and resolution $J = 4$ was taken for figure 4.2

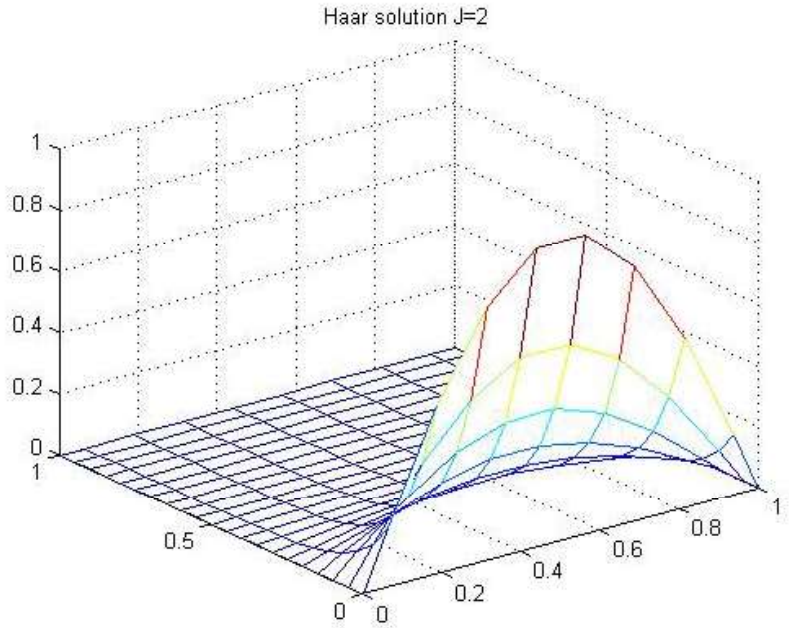

Figure 4.1: Solution of example using Haar collocation method with J=2.

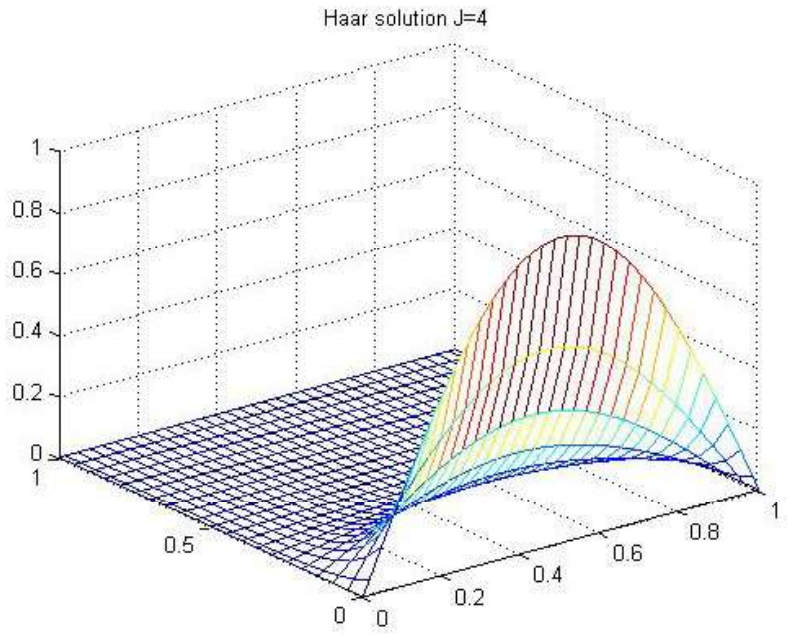

Figure 4.2: Solution of example using Haar collocation method with J=4.

4.4 Convergence of Haar wavelet series

Let $u(x) \in L^2(R)$ and let $\sum_{i=1}^{\infty} a_i \psi_i(x)$ be its wavelet series where $\psi_i's$ are defined in chapter 2 article 2.1.3 equation 2.1.13. The following result assures the convergence of wavelet series. We define error e_j with resolution j as $u - u_j$ where

$$u_j = \sum_{i=1}^{2^{j+1}} a_i \psi_i(x).$$

Result: For $u(x) \in L^2(R)$, the error norm with resolution j is bounded and

$$\|e_j(x)\| \leq \sqrt{\frac{K_1}{7}} C_1 2^{-(3)2^{j-1}}$$

where K_1 and C_1 are obtained by

$$\max|u'(x)| \leq K_1 \quad and \quad C_1 = \int_0^1 |x\psi_2(x)|dx$$

as in [39], [90], [62] , which is verified in the example solved with $J = 4$ and $J = 2$ in chapter 3.

Proof: Consider j as the assumed resolution level

$$\begin{aligned} &|e_j(x)| = |u - u_j(x)| = \left|\sum_{i=2^{j+1}+1}^{\infty} a_i\psi_i(x)\right| \\ &where \quad u_j(x) = \sum_{i=1}^{2^{j+1}} a_i\psi_i(x) \\ &Now \quad \|e_j(x)\|^2 = \sum_{i=2^{j+1}+1}^{\infty}\sum_{l=2^{j+1}+1}^{\infty} a_i a_l \int_{-\infty}^{\infty} \psi_i(x)\psi_l(x)dx \end{aligned} \tag{4.4.1}$$

Hence now

$$\|e_j(x)\|^2 \leq \sum_{i=2^{j+1}+1}^{\infty} |a_i|^2 \tag{4.4.2}$$

But

$$|a_i| \leq C_1 2^{-\frac{3}{2}i} \max|u'(\eta)| \tag{4.4.3}$$

where $C_1 = \int_0^1 |x\psi_2(x)|dx \quad and \quad \eta \in (k2^{-j}, (k+1)2^{-j})$ hence

$$\begin{aligned} &\|e_j(x)\|^2 \leq \sum_{i=2^{j+1}+1}^{\infty} K_1 C_1^2 2^{-3i} \\ &where \quad |u'(x)| < K_1 \\ &and \quad hence \, \|e_j(x)\| \leq \sqrt{\tfrac{K_1}{7}} C_1 2^{-3(2)^{j-1}} \end{aligned} \tag{4.4.4}$$

4.5 Observations

The orthogonal property of Haar wavelet used as basis reduces the computational cost, just by increasing the resolution. Higher accuracy is obtained in the solution which is shown in tables 4.1 and table 4.2. This provides a solid foundation in application of Haar wavelet to partial differential equation. Table 4.3 compares the approach of Haar wavelet collocation with finite difference method and indicates the improvement of solution in absolute sense.

4.6 Elliptic partial differential equation

4.6.1 Algorithm-EPDE

The definition of Haar wavelet and multi resolution as [58] are utilized. The approach includes the consideration of second order derivative as Haar approximations in both x and y direction as

$$w_{xx} = H^T(x)C_1H(y) \tag{4.6.1}$$

$$w_{yy} = H^T(x)C_2H(y) \tag{4.6.2}$$

For the elliptic partial differential equation was taken to be,

$$w_{xx} + w_{yy} = 0 \tag{4.6.3}$$

where C_1 and C_2 represent the coefficient matrix of dimension m. Now integrating equation 4.6.1 twice with respect to x and y between 0 to x and 0 to y respectively

we obtain,

$$w_x(x,y) = H^T Q_H^T C_1 H(y) + w_x(0,y) \tag{4.6.4}$$

$$w(x,y) = H^T Q_H^T Q_H^T C_1 H(y) + x w_x(0,y) + w(0,y) \tag{4.6.5}$$

and

$$w_y(x,y) = H^T Q_H^T C_2 H(y) + w_y(x,0) \tag{4.6.6}$$

$$w(x,y) = H^T Q_H^T Q_H^T C_2 H(y) + y w_y(x,0) + w(x,0) \tag{4.6.7}$$

The procedure includes assuming the highest derivative term as linear combination of Haar wavelet and the successive integration is performed to obtain the original function. The terms are substituted into the governing equation to be solved which leads us to solve only system of algebraic equation in Haar coefficients.

4.6.2 Numerical examples

The cases discussed in this study include different boundary conditions for

$$w_{xx} + w_{yy} = 0 \tag{4.6.8}$$

and Helmholtz equation handled for the described approach as follows:

4.6.3 Case 1

Here the equation 4.6.8 is solved with,

$$\begin{aligned} w(x,0) &= 2x(1-x) \\ w(x,1) &= w(0,y) = w(1,y) = 0 \end{aligned} \tag{4.6.9}$$

4.6.4 Case 2

The equation 4.6.8 is solved with,

$$\begin{aligned} w(x,0) &= x \\ w(x,1) &= x^2 - 1, \\ w(0,y) &= -y^2, \\ w(1,y) &= -y^2 \end{aligned} \tag{4.6.10}$$

4.6.5 Case 3

Here the equation 4.6.8 is solved with,

$$\begin{aligned} w(x,0) &= x^2, \\ w(x,1) &= x^2 - 1, \\ w(0,y) &= -y^2, \\ w(1,y) &= 1 - y^2 \end{aligned} \tag{4.6.11}$$

4.6.6 Case 4 Helmholtz equation

Consider the Helmholtz equation as

$$w_{xx} + w_{yy} = f(x, y) \tag{4.6.12}$$

with boundary conditions

$$\begin{aligned} w(x, 0) &= 0, \\ w(x, 1) &= 0, \\ w(0, y) &= 0, \\ w(1, y) &= 0, \\ f(x, y) &= (k - 2\pi^2) \sin(\pi x) \sin(\pi y). \end{aligned} \tag{4.6.13}$$

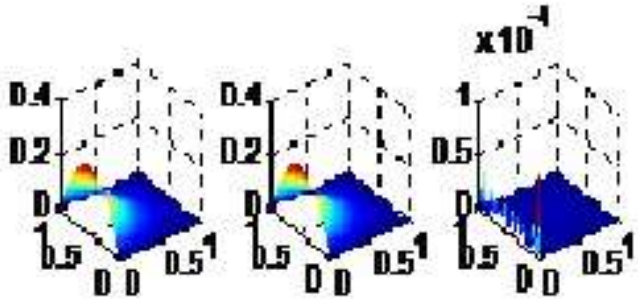

Figure 4.3: Error plot for case 1

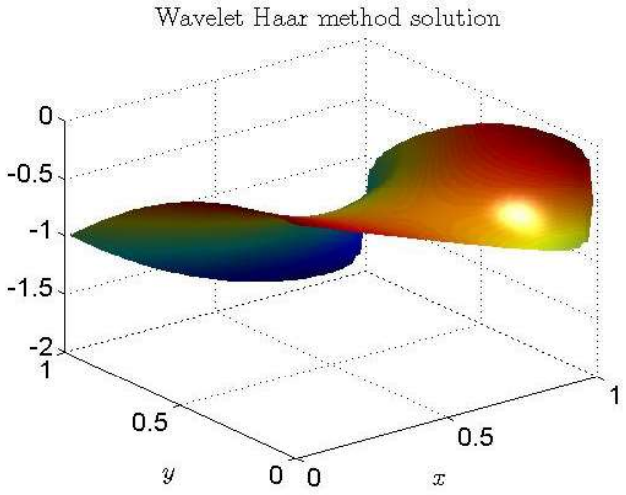

Figure 4.4: Haar solution for case 2

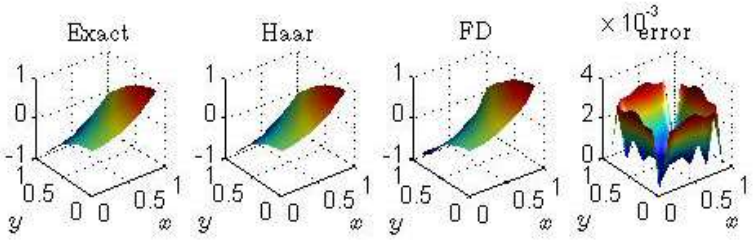

Figure 4.5: Comparison of exact, Haar and FDM for case 3

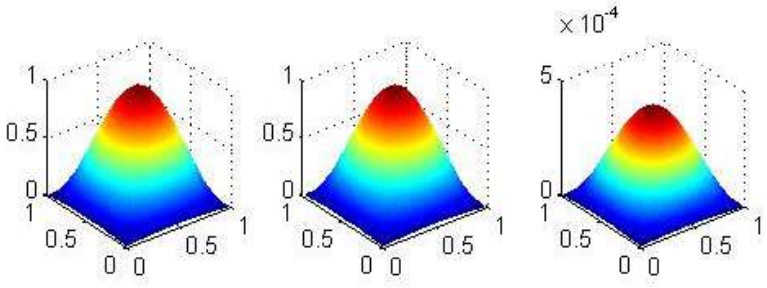

Figure 4.6: Comparison of solution of Helmholtz equation using exact, Haar, percentage error.

Error plots are analyzed to observe that error is sufficiently reduced using the Haar approach. In case 1 given by equation 4.6.9, 128 grid points are considered. Figure 4.3 shows comparison of exact solution, Haar solution along with the percentage error plots from left to right respectively. Figure 4.4 gives the Haar solution for case 2. For case 3 given by equation 4.6.11, the solution is given in figure 4.5 which compares the exact solution, Haar solution, finite difference and percent error of Haar solution. For case 3, m is taken to be 8. Figure 4.6 compares the solution of Helmholtz equation 4.6.12 with $k = 0.5$. It gives the comparison of exact, Haar solution along with percentage error from left to right taking $m = 64$.

4.7 Convergence analysis of two dimensional wavelet method:

Assuming that, $f(x,y) \in C^2([q,r] \times [q,r])$ there exist $M > 0$, for which,

$$|\frac{\partial^2 f(x,y)}{\partial x \partial y}| \leq M, \quad \forall \quad x,y \in [q,r] \times [q,r]$$

Considering

$$f_{nm}(x,y) = \sum_{i=0}^{n-1} \sum_{j=0}^{m-1} a_{ij} \psi_i(x) \psi_j(y)$$

where $n = 2^{\alpha+1}, \quad \alpha = 0,1,2,\cdot\cdot \quad m = 2^{\beta+1}, \quad \beta = 0,1,2,\cdot\cdot$ then [93]

$$\|f(x,y) - f_{kl}(x,y)\| \leq \frac{(b-a)^{10} M^2}{3} \Big(\frac{1}{3l^2k^2 + \frac{13}{21k^2} + \frac{13}{21l^2}} \Big).$$

As $l \to \infty$ and $k \to \infty$ leads to

$$\|f(x,y) - f_{kl}(x,y)\| \to 0.$$

for $k < n, \quad l < m.$

4.8 Observations

Different cases with boundary conditions are analyzed at different resolutions, which shows the significance of the approach used. It clearly indicates that a very fine change in resolution gives a better approximation. The plots as in figure 4.3 and 4.5 which compares the Haar wavelet approach with solutions using exact and finite difference method with the percentage error as low as 2.